Immunity, Vol. 10, 473–483, April, 1999, Copyright ©1999 by Cell Press

Role of the T Cell Receptor α Chain in Stabilizing TCR-Superantigen-MHC Class II Complexes

Peter S. Andersen,* Pascal M. Lavoie,† Rafick-Pierre Sékaly,† Hywyn Churchill,‡ David M. Kranz,‡ Patrick M. Schlievert,§ Klaus Karjalainen,‖ and Roy A. Mariuzza*#
*Center for Advanced Research in Biotechnology
University of Maryland Biotechnology Institute
9600 Gudelsky Drive
Rockville, Maryland 20850
†Laboratoire d'Immunologie
Institut de Recherches Cliniques de Montréal
110 avenue des Pins Ouest
Montréal, Québec H2W 1R7
Canada
‡Department of Biochemistry
University of Illinois
Urbana, Illinois 61801
§Department of Microbiology
University of Minnesota Medical School
Minneapolis, Minnesota 55455
‖Basel Institute for Immunology
Grenzacherstrasse 487
Postfach CH-4005, Basel
Switzerland

Summary

Superantigens (SAGs) activate T cells by simultaneously binding the Vβ domain of the TCR and MHC class II molecules on antigen-presenting cells. The preferential expression of certain Vα regions among SAG-reactive T cells has suggested that the TCR α chain may modulate the level of activation through an interaction with MHC. We demonstrate that the TCR α chain is required for maximum stabilization of the TCR-SAG-MHC complex and that the α chain increases the half-life of the complex to match those of TCR-peptide/MHC complexes. The site on the TCR α chain responsible for these effects is CDR2. Thus, the overall stability of the TCR-SAG-MHC complex is determined by the combination of three distinct interactions: TCR-SAG, SAG-MHC, and MHC-TCR.

Introduction

Superantigens (SAGs) are a class of immunostimulatory and disease-causing proteins of viral or bacterial origin with the ability to activate large fractions (5%–20%) of the T cell population. SAGs include self-antigens, such as the minor lymphocyte-stimulating antigens (Mls) encoded by endogenous murine retroviruses, as well as foreign antigens, such as staphylococcal and streptococcal pyrogenic toxins (Bohach et al., 1990; Kotzin et al., 1993; Scherer et al., 1993; Webb and Gascoigne, 1994; Bohach, 1997). T cell activation by SAGs requires simultaneous interaction of the SAG with the TCR and with MHC class II molecules on an antigen-presenting cell (APC). Immunological (Kotzin et al., 1993; Scherer et al., 1993; Webb and Gascoigne, 1994), X-ray crystallographic (Fields et al., 1996; Li et al., 1998, 1999), and direct binding (Gascoigne and Ames, 1991; Malchiodi et al., 1995) studies have demonstrated that T cell reactivity to microbial SAGs is primarily determined by the TCR Vβ element. Indeed, staphylococcal enterotoxins B and C3 (SEB and SEC3) contact only complementarity-determining region 2 (CDR2), framework regions 2 and 3 (FR2 and FR3), and hypervariable region 4 (HV4) of the TCR β chain, with no direct involvement of the TCR α chain (Li et al., 1999).

Despite the dominant role of Vβ in SAG recognition, there is increasing evidence that non-Vβ elements may also affect reactivity (Woodland and Blackman, 1993; Webb and Gascoigne, 1994; Daly et al., 1995; Blackman and Woodland, 1996; Donson et al., 1997). For example, endogenous expression of Mls-1 resulted in only partial (~50%) thymic clonal deletion in mice transgenic for the strongly Mls-1-reactive Vβ8.1 β chain, suggesting an influence of the nontransgenic α chains with which the transgenic β chain had paired (Blackman et al., 1990). An analysis of Vβ8.1$^+$ T cell hybridomas from Mls-1$^-$ mice in which Mls-1-reactive T cells were not deleted revealed a skewing of α chain usage between Mls-1-reactive and Mls-1-nonreactive hybridomas, such that hybridomas expressing Vα11.1 were biased toward Mls-1 reactivity, whereas hybridomas expressing Vα2, Vα8, or Vα11.3 were biased against reactivity (Smith et al., 1992). These Vβ8.1$^+$ hybridomas exhibited a similar pattern of α chain bias in their reactivity toward SEB. Similarly, Borrero et al. (1995) found that Vα4 is expressed by Vβ6$^+$ T cell hybridomas that react with SEB but not by Vβ6$^+$ hybridomas that do not respond to this SAG. Transfection experiments demonstrated that the Vα4 α chain transferred SEB responsiveness regardless of whether the Vβ6 β chain was derived from a responsive or nonresponsive hybridoma (Donson et al., 1997). The preferential expression of certain Vα regions among SAG-reactive T cells, along with evidence of a functional interaction between the TCR α chain and MHC class II in the TCR-SAG-MHC complex (Deckhut et al., 1994; Labrecque et al., 1994), has been interpreted as an indication that these particular Vαs interact with MHC more favorably than other Vαs during SAG-mediated T cell activation (Woodland and Blackman, 1993; Webb and Gascoigne, 1994; Blackman and Woodland, 1996; Donson et al., 1997).

To help explain the observed influence of the TCR α chain on SAG reactivity, we have constructed models of the TCR-SEC3-peptide/MHC class II complex based on the crystal structures of the VβCβ-SEC3 (Fields et al., 1996) and VβCβ-SEB (Li et al., 1998) complexes, the SEB-peptide/HLA-DR1 complex (Jardetzky et al., 1994), and several different TCR αβ heterodimers (Garboczi et al., 1996; Garcia et al., 1996; Housset et al., 1997; Wang

To whom correspondence should be addressed (e-mail: mariuzza@indigo2.carb.nist.gov).

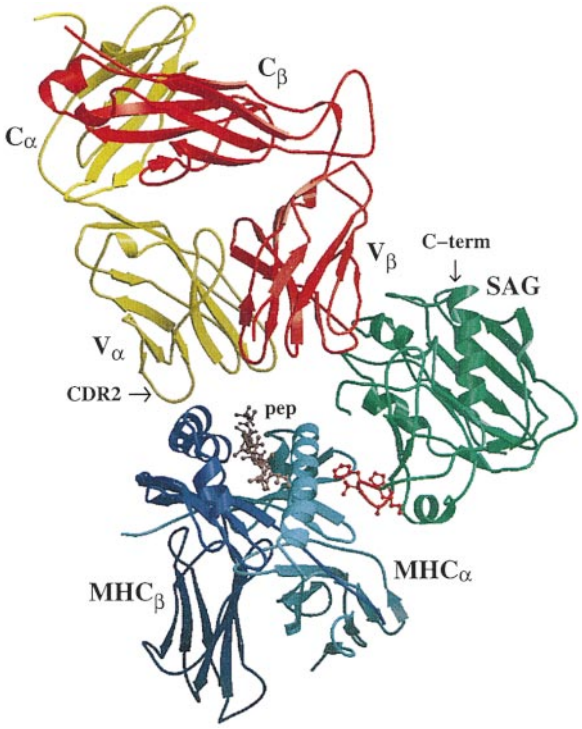

Figure 1. Model of the TCR-SEC3-Peptide/MHC Class II Complex

The model was constructed according to Li et al. (1998) by least-squares superposition of the 14.3.d VβCβ-SEC3 complex (Fields et al., 1996), the SEB-peptide/HLA-DR1 complex (Jardetzky et al., 1994), and the 2C TCR VαCα/VβCβ heterodimer (Garcia et al., 1998), which uses the same Vβ element (mouse Vβ8.2) as the 14.3.d TCR. The CDR2 loop of the 2C Vα domain is labeled. The C terminus of SEC3, used for attachment to bacteriophage gene III protein (see text), is indicated. The 44–47 loop (KFLAH) of SEC3 that was targeted for saturation mutagenesis is shown in red with side chains included. Models (data not shown) of the TCR-SEC3-peptide/MHC class II complex were also constructed using TCRs A6 (Garboczi et al., 1996) and N15 (Wang et al., 1998). In both cases, the putative contacts between the TCR and the MHC β1 helix are mediated by Vα CDR2, despite differences in Vα/Vβ domain orientation and Vα CDR2 loop structure (Li et al., 1998).

et al., 1998). As shown in Figure 1, the models predict that the Vα domain interacts with the MHC β1 helix through its CDR2 loop, suggesting that TCR-MHC contacts may help stabilize the TCR-SAG-MHC complex. However, the extent of the Vα-MHC interaction is variable and depends on the geometry of Vα/Vβ domain association and on the structure of the Vα CDR2 loop (Li et al., 1998). We hypothesized that this variability, by stabilizing the TCR-SAG-MHC complex to different degrees, could account for the preferential expression of certain Vα regions among T cells reactive with a particular SAG. However, no direct proof of a stabilizing effect of the TCR α chain on ternary complex formation has been reported.

The high efficiency with which SAGs trigger T cells, which is comparable to the efficiency of activation by specific peptide/MHC complexes (Viola and Lanzavecchia, 1996), presents a paradox. With affinities for both TCR and MHC class II in the micromolar range (Li et al., 1999), it is difficult to understand how SAGs can effectively cross-link the T cell and APC at the nanomolar concentrations commonly employed in T cell stimulation assays, since the vast majority of SAG molecules should be unbound under these conditions (Proft and Fraser, 1998). The problem is less severe for peptide/MHC because the peptide is, in effect, irreversibly bound to the MHC molecule. Thus, some mechanism(s) must exist to permit SAGs to trigger T cells at concentrations orders of magnitude below their dissociation constants (K_Ds) for TCR or MHC. One possibility is that accessory molecules such as CD4 help stabilize the TCR-SAG-MHC complex sufficiently for activation to occur. However, T cell stimulation by bacterial SAGs is largely independent of CD4 or CD8 (Kotzin et al., 1993). Another possibility is that the overall stability of the TCR-SAG-MHC complex is considerably greater than would be expected from considering the TCR-SAG and SAG-MHC interactions independently. That is, the binding of SAGs may be a cooperative process in which the SAG-MHC complex binds the TCR with greater affinity than does the SAG alone or in which the TCR-SAG complex binds MHC with greater affinity than does the free SAG. Cooperativity may occur in one of several ways: binding of the SAG to MHC induces a conformational change in the SAG that increases its affinity for the TCR, binding of the SAG to TCR induces a conformational change in the SAG that increases its affinity for MHC, or TCR-MHC interactions occur in the TCR-SAG-MHC complex that, combined with TCR-SAG and SAG-MHC interactions, contribute to its overall stabilization. With respect to possible conformational changes upon binding, X-ray crystallographic studies of SAG-MHC (Jardetzky et al., 1994; Kim et al., 1994; Dessen et al., 1997) and TCR β chain-SAG (Fields et al., 1996; Li et al., 1998) complexes have revealed that there are no major structural rearrangements in any of the individual components as a result of complex formation that could increase the affinity of the SAG for TCR or MHC. On the other hand, the model in Figure 1 predicts that the TCR Vα domain may interact with the MHC β1 helix, thereby potentially increasing the stability of the TCR-SAG-MHC complex to match that of the TCR-peptide/MHC complex.

To investigate the possible role of the TCR α chain in stabilizing the TCR-SAG-MHC complex, we have measured the binding of SEC3 to recombinant forms of two different TCRs in the presence and absence of a human MHC class II molecule, HLA-DR1. We show that soluble HLA-DR1 significantly enhances the binding of SEC3 to the αβ TCR heterodimers but has no effect on the binding of SEC3 to the TCR β chain alone. We find that the TCR α chain increases the half-life of the TCR-SEC3-DR1 complex to a value comparable to those reported for specific TCR-peptide/MHC class I or class II complexes (1–60 s) (Corr et al., 1994; Matsui et al., 1994; Alam et al., 1996; Lyons et al., 1996; Kersh et al., 1998). Using phage display technology to isolate variants of SEC3 with up to 60-fold tighter binding to HLA-DR1, we show that increasing the affinity of the SAG-MHC interaction further extends the half-life of the ternary complex, as predicted by a model involving direct TCR-MHC interactions. Finally, we have used site-directed mutagenesis to identify Vα CDR2 as the apparent site on the TCR α chain responsible for maximizing the stability of the TCR-SAG-MHC complex.

Results and Discussion

The TCR α Chain Stabilizes the TCR-SAG-MHC Complex

A previous BIAcore study showed that the binding of SEB to an immobilized human TCR is significantly increased by the addition of soluble HLA-DR1 (Seth et al., 1994), suggesting that the affinity of the TCR for SEB complexed with MHC class II is greater than its affinity for the SAG alone. To determine the structural basis for this effect, we utilized soluble forms of the associated 14.3.d αβ TCR (mouse Vα4.1/Vβ8.2) and of the isolated 14.3.d β chain. The αβ heterodimer was secreted by *Drosophila* cells transfected with α and β chains truncated before their transmembrane regions, while the unpaired β chain was expressed by myeloma cells transfected with truncated β chain alone (Bentley et al., 1995). As a source of MHC class II, we used soluble HLA-DR1 produced by Sf21 insect cells infected with a recombinant baculovirus encoding truncated DRα and DRβ chains (Stern and Wiley, 1992; Murthy and Stern, 1997). The empty class II molecules were loaded with either influenza virus hemagglutinin peptide 306-318 (HA 306-318) or with the YAK peptide (Natarajan et al., 1999), a derivative of HA 306-318 bearing multiple alanine substitutions.

To determine if simultaneous binding of 14.3.d TCR and HLA-DR1 to SEC3 leads to enhanced stability of the TCR-SAG-MHC complex, soluble TCR, soluble HLA-DR1/HA 306-318, and a mixture of the two were injected over immobilized SEC3 (Figure 2A). To estimate the increase in resonance units (RU) resulting from the nonspecific effect of protein on the bulk refractive index, the binding of TCR and MHC to a control surface with no immobilized SAG was also measured (Figure 2A). No specific binding of HLA-DR1 was detectable at the concentration used in the assay (1.5 μM), as expected from our estimate of 270 μM for the K_D of the SEC3-DR1 interaction (see below). On the other hand, the TCR heterodimer at a concentration of 12 μM produced a significant response, consistent with the affinity of the 14.3.d β chain for SEC3 (K_D = 3.0 μM) (Leder et al., 1998). The signal for the mixture of TCR and MHC was significantly greater than the sum of the individual responses, as also reported for SEB (Seth et al., 1994). Moreover, the dissociation kinetics were clearly slower for the mixture of TCR and MHC than for TCR alone (Figure 2A). Identical results were obtained using HLA-DR1 loaded with YAK, showing that the effect is not peptide specific. To ascertain whether the increased signal and decreased off-rate were dependent on the TCR α chain, we repeated the experiment, but this time replacing the 14.3.d TCR heterodimer with the corresponding soluble β chain. As seen in Figure 2B, the response elicited by the mixture of 14.3.d β chain and HLA-DR1 did not exceed the sum of the responses to the two proteins when injected individually. The rapid dissociation kinetics of β chain binding to SEC3 were likewise unaltered by the inclusion of soluble MHC class II.

Protein aggregation in the relatively dense dextran matrix of the sensor chip can present serious difficulties in the interpretation of BIAcore results (Davis et al., 1998). Indeed, the sensogram for the binding of soluble 14.3.d TCR to immobilized SEC3 clearly shows signs of aggregation: biphasic association (a fast initial increase of about 375 RU followed by a much slower increase of about 50 RU) and elevated baseline upon washing (Figure 2A). To rule out the possibility that aggregation of the 14.3.d TCR is somehow responsible for the enhanced binding to immobilized SEC3 observed in the presence of HLA-DR1, the orientation of the assay was reversed.

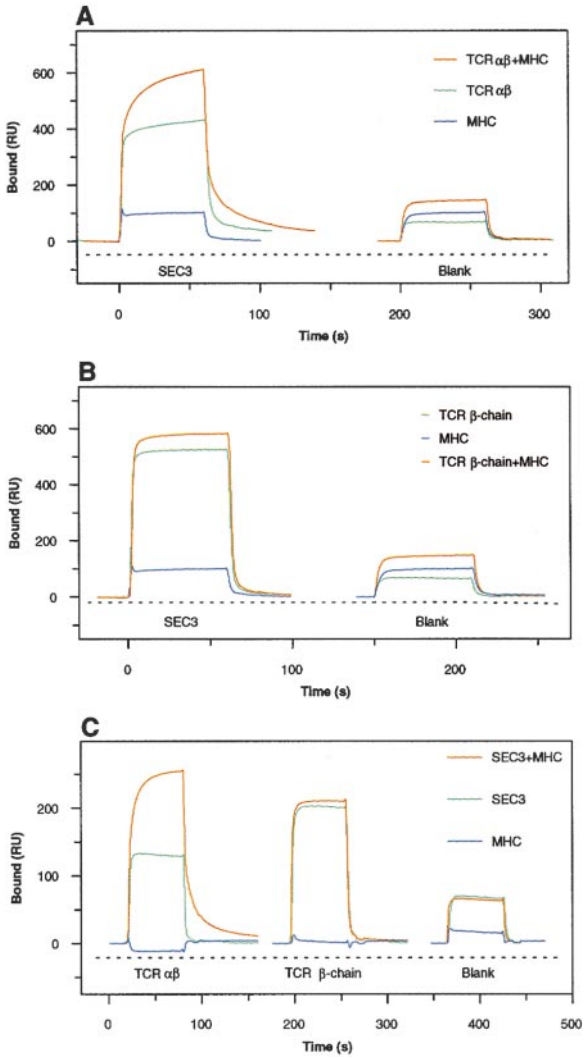

Figure 2. BIAcore Analysis of TCR and MHC Binding to SEC3

(A) Sensograms of 12 μM 14.3.d αβ TCR (green), 1.5 μM soluble HLA-DR1 (blue), or 12 μM 14.3.d αβ TCR and 1.5 μM HLA-DR1 (red) injected over a surface coupled with SEC3 (1100 RU, approximately 80% active) or over a blank control surface, as indicated below each overlay plot.

(B) Sensograms of 19 μM 14.3.d TCR β chain (green), 1.5 μM soluble HLA-DR1 (blue), or 19 μM 14.3.d TCR β chain and 1.5 μM HLA-DR1 (red) injected over a surface coupled with SEC3 (1100 RU, approximately 80% active) or over a blank control surface.

(C) Sensograms of 6 μM SEC3 (green), 2.5 μM soluble HLA-DR1 (blue), or 6 μM SEC3 and 2.5 μM HLA-DR1 (red) injected over immobilized 14.3.d αβ TCR (3000 RU, approximately 60% active), 14.3.d TCR β chain (2400 RU, about 40% active), or over a blank control surface. The percentage of active αβ TCR or TCR β chain was estimated by Scatchard analysis using SEC3.

Thus, we immobilized the TCR instead of the SAG and repeated the above experiments using SEC3, soluble HLA-DR1, and a combination of the two. There are no signs of significant aggregation in the binding of SEC3 to immobilized 14.3.d TCR: the equilibrium binding level was reached within seconds and the response rapidly returned to baseline upon completion of the injection (Figure 2C). Furthermore, the affinity of the immobilized $\alpha\beta$ TCR for SEC3, as measured by Scatchard analysis under equilibrium binding conditions, was indistinguishable from that of the immobilized 14.3.d β chain alone, approximately 20 μM (data not shown), consistent with the predicted lack of direct contacts between SEC3 and the TCR α chain in the TCR β-SEC3 complex (Fields et al., 1996). However, the binding of SEC3 to immobilized TCR was markedly enhanced by soluble HLA-DR1, such that the response to a mixture of SEC3 and DR1 was approximately twice the sum of the responses to the individual components. The apparent off-rate was also decreased, compared with that for the binding of SEC3 alone to TCR. Injecting the same samples over immobilized 14.3.d β chain confirmed the requirement of the TCR α chain for the formation of complexes with increased stability, since the sensogram obtained by injecting SEC3 alone is nearly superimposable on that obtained by injecting the mixture of SEC3 and HLA-DR1 (Figure 2C). These results are in agreement with those obtained using immobilized SAG and are therefore independent of the orientation of the assay. Similar results were obtained using SEB (data not shown).

The effect of the TCR α chain in stabilizing the TCR-SAG-MHC complex may be understood in terms of the model in Figure 1 in which the Vα domain of the TCR is predicted to interact with the MHC β1 helix. This suggests that the overall stability of the complex is determined by the interplay of three distinct interactions: TCR β chain-SAG, SAG-MHC α chain, and MHC β chain-TCR α chain. A test of this hypothesis was designed as follows.

The formation of a ternary complex involving three different components (e.g., TCR, SAG, and MHC) may occur by one of two general mechanisms. In the simpler case, only one of the three components is able to bind, or cross-link, the other two. Alternatively, each of the three components can form productive interactions with the other two. In principle, it is possible to discriminate between these mechanisms by examining the effects of altering the affinity of individual interactions on the stability of the overall complex. For example, if the TCR-SAG-MHC complex is formed by the SAG simply cross-linking TCR and MHC (TCR-SAG and SAG-MHC interactions only, with no TCR-MHC interaction), increasing the affinity of the SAG-MHC interaction should not affect the half-life of the ternary complex, as measured in a BIAcore assay in which the TCR is immobilized, since the affinity of the TCR for the SAG-MHC complex will be the same as its affinity for the free SAG. If, on the other hand, TCR-MHC interactions contribute to stabilizing the TCR-SAG-MHC complex, increasing the affinity of the SAG-MHC interaction should increase the half-life of the ternary complex since, in this case, the affinity of the TCR for the SAG-MHC complex will be greater than its affinity for the SAG alone. We have tested this prediction by using phage display technology to isolate mutants of SEC3 with increased affinity for MHC and by comparing the ability of these mutants to stabilize the TCR-SAG-MHC complex with that of the wild-type SAG.

Isolation of SEC3 Variants with Increased Affinity for HLA-DR1 from a Phage Display Library

The high degree of sequence homology between SEB and SEC3 (65% identical), their very similar three-dimensional structures (Swaminathan et al., 1992; Hoffmann et al., 1994), and the nearly identical ways in which they bind TCR (Fields et al., 1996; Li et al., 1998) make it reasonable to assume that SEB and SEC3 possess similar binding sites for MHC class II. In the structure of the SEB-HLA-DR1 complex (Jardetzky et al., 1994), SEB binds to the α1 domain of DR1. The interface displays two main structural features: a salt bridge between SEB residue Glu67 and DR1 α chain residue Lys39 and a protruding hydrophobic loop composed of SEB residues 43–47 (QFLYF) that fits into a predominantly hydrophobic depression on the α1 domain of DR1 formed by the first and third turns of the β sheet and the N-terminal portion of the α-helix (Figure 1). The glutamic acid at SEB position 67 is conserved (or conservatively substituted) in SEC1–3, SEA, SED, SEE, SPEA, SPEC, and SSA, whereas the sequence of the 44–47 loop is more variable. We therefore targeted the corresponding region of SEC3 (KFLAH) for saturation mutagenesis in search of variants with increased affinity for HLA-DR1. A library of approximately 1.3×10^7 unique clones was displayed on the surface of filamentous bacteriophage by fusion to the N terminus of gene III protein (see Experimental Procedures for details). In the structure of the SEB-HLA-DR1 complex (Jardetzky et al., 1994), the C terminus of the SAG is distant from the MHC combining site (Figure 1); consequently, attachment of gene III protein at this position should not interfere with MHC binding. The phage library was selected by panning on immobilized HLA-DR1. Several clones with increased reactivity toward this MHC were identified, and two with either medium (SEC3 3B1) or high (SEC3 3B2) reactivity were chosen for further characterization. Their amino acid sequences at positions 43–47 are shown in Figure 3D. Soluble protein was produced for each mutant by transfecting phagemid DNA into a nonsuppressor *Escherichia coli* strain, ensuring translation of only the SEC3 part of the SEC3-gene III fusion (Hoogenboom et al., 1991). The affinities of the SEC3 mutants for HLA-DR1 were measured by BIAcore (Figures 3A and 3B). Because we were unable to directly couple DR1 to the sensor surface with satisfactory retention of SAG-binding activity, we first coupled SEA to the matrix and then used its Zn^{2+}-dependent, high-affinity binding site for the DR1 β chain (Abrahmsen et al., 1995; Hudson et al., 1995; Kozono et al., 1995) to capture the MHC molecule. This site is distinct from the low-affinity SEC3 site on the DR1 α chain, such that one SEA molecule can simultaneously bind two SAG molecules (Tiedemann et al., 1995). Wild-type SEC3 and SEC3 mutants were injected over a range of concentrations and concentration-dependent binding profiles recorded (Figure 3A). Affinities for HLA-DR1 were determined by Scatchard analysis under equilibrium binding conditions (Figure 3B). The

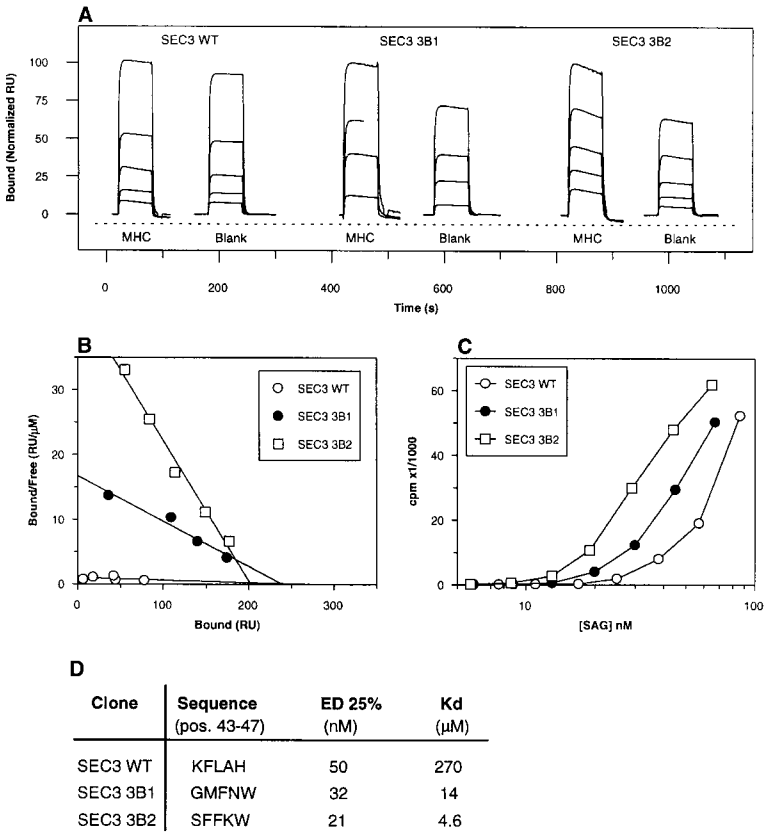

D

Clone	Sequence (pos. 43-47)	ED 25% (nM)	Kd (μM)
SEC3 WT	KFLAH	50	270
SEC3 3B1	GMFNW	32	14
SEC3 3B2	SFFKW	21	4.6

Figure 3. Characterization of SEC3 Mutants with Increased Affinity for MHC Class II Selected from a Phage Display Library

(A) Sensograms showing binding of wild-type SEC3 (SEC3 WT), SEC3 3B1, and SEC3 3B2 to immobilized HLA-DR1 or to a control surface. Initial concentrations of the SAGs (SEC3 WT, 130 μM; SEC3 3B1, 42 μM; and SEC3 3B2, 27 μM) were serially diluted 2-fold, and samples at four or five different concentrations were injected over HLA-DR1 bound to SEA through its high-affinity site for the DR1 β chain. The control (blank) was the SEA-coupled surface prior to the injection of HLA-DR1. Due to differences in the amount of bound MHC at the time of injection, all sensograms were normalized to facilitate comparisons.

(B) Scatchard analysis of the binding of SEC3 WT, SEC3 3B1, and SEC3 3B2 to HLA-DR1 with data derived from (A) after correction for the bulk effect. The data were fitted to straight lines; K_Ds were calculated directly from the slopes.

(C) Proliferation of lymph node T cells from RAG2$^{-/-}$ 14.3.d TCR transgenic mice in the presence of SEC3 WT, SEC3 3B1, or SEC3 3B2. Mouse fibroblasts transfected with genes encoding HLA-DR1 were used as APCs. The SAG concentrations are indicated with the different symbols. Proliferation results at 48 hr are shown here. The results were qualitatively the same at 72 hr.

(D) Table showing the sequences of wild-type and mutant SEC3 proteins at positions 43–47. The K_Ds for binding to HLA-DR1, determined from the Scatchard plots in (B), are given. The effective dose (ED) of each SAG is expressed as the concentration (nM) required to induce 25% of maximum T cell proliferation in (C).

K_Ds for the binding of SEC3 3B1 and SEC3 3B2 were 14 and 4.6 μM, respectively, compared with 270 μM for wild-type SEC3. Thus, SEC3 3B1 and SEC3 3B2 bind HLA-DR1 approximately 20- and 60-fold more tightly, respectively, than the wild-type protein. The affinities of the mutants for the 14.3.d TCR were similar to that of wild-type SEC3. The abilities of SEC3 3B1 and SEC3 3B2 to induce proliferation of resting lymph node T cells bearing the 14.3.d TCR from RAG-2$^{-/-}$ TCR transgenic mice were measured using mouse fibroblasts expressing HLA-DR1 as APCs (Figure 3C). The results, expressed as the dose of each SAG required to induce 25% of maximum T cell proliferation, show that mitogenic potency increases with increasing affinity for MHC (Figure 3D), in agreement with previous results (Leder et al., 1998).

Kinetic Analysis of TCR-SAG-MHC Complex Formation as a Function of SAG-MHC Affinity

To determine if the increase in MHC affinity had the predicted effect on the stability of the TCR-SAG-MHC complex, wild-type SEC3, SEC3 3B1, and SEC3 3B2 were injected over immobilized 14.3.d TCR, either alone or premixed with 1 μM soluble HLA-DR1 (Figure 4A). Both mutants displayed greater degrees of enhanced binding than the wild-type SAG. Moreover, there was a correlation between MHC affinity and the amount of enhancement, such that SEC3 3B2 (K_D = 4.6 μM) showed significantly more complex formation than SEC3 3B1 (K_D = 14 μM). In order to rule out the possibility that the enhanced binding we observed for SEC3 3B1 and SEC3 3B2 is simply due to increased binding of MHC to the mutant SAGs bound to immobilized TCR, independently of any TCR-MHC interaction, we repeated the experiment using immobilized 14.3.d β chain alone (data not shown). In this case, injection of SEC3 3B1 or SEC3 3B2 premixed with DR1 gave the same result as injection of wild-type SEC3 premixed with DR1, with no increase in complex formation. This is in fact consistent with the affinities of the mutants for DR1: even for SEC3 3B2 (K_D = 4.6 μM), one may calculate that only 7% of the SAG molecules would be complexed with MHC at the concentrations employed if the SAG simply cross-linked TCR and MHC in the absence of any TCR-MHC interactions, such that MHC would have only a relatively small effect on the total response (a 12% increase in RU compared with the approximately 300% increase actually observed).

A visual comparison of the dissociation phases in Figure 4A suggested that increasing the affinity of the SAG-MHC interaction also increased the half-life of the TCR-SAG-MHC complex, as predicted above. To determine whether this was indeed the case, we measured the off-rates for the ternary complexes formed by wild-type SEC3 (Figure 4B) and by SEC3 3B2 (Figure 4C). Fixed concentrations of each SAG (3 μM for wild-type SEC3 and 6 μM for the mutant) were injected over immobilized 14.3.d TCR in combination with increasing

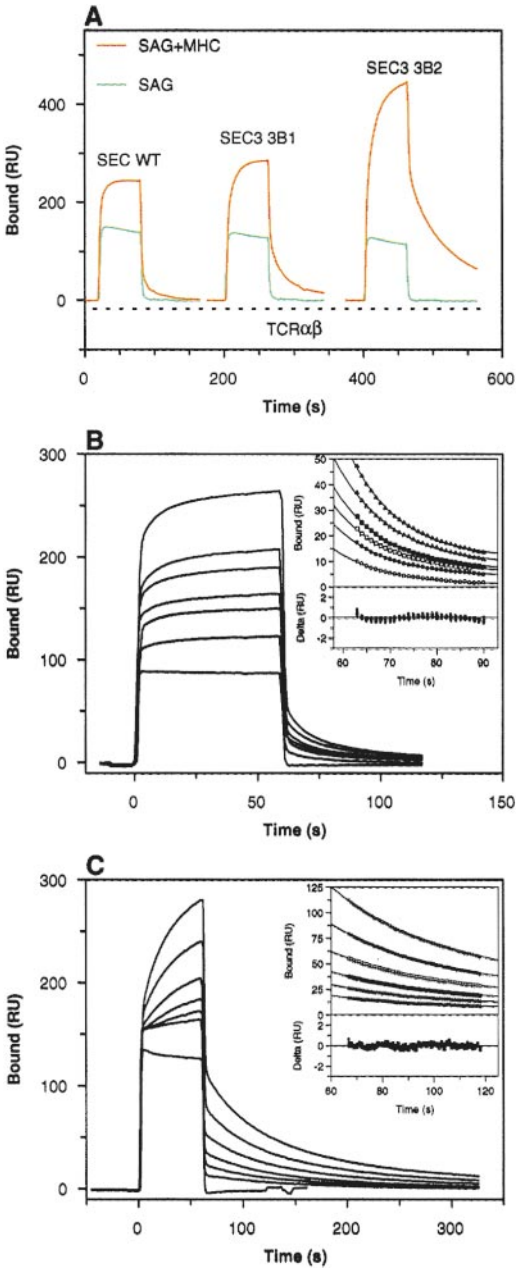

Figure 4. Effects of the Affinity of the SAG-MHC Interaction on Stability of the TCR-SAG-MHC Complex

(A) Sensograms showing the binding of wild-type SEC3 (SEC3 WT), SEC3 3B1, and SEC3 3B2 to immobilized 14.3.d αβ TCR in the presence or absence of soluble HLA-DR1. 8 μM SEC3 WT, 6 μM SEC3 3B1, or 6 μM SEC3 3B2 was injected over 3000 RU of immobilized 14.3.d TCR, either alone (green) or mixed with 1.0 μM HLA-DR1 (red).

(B) Determination of the off-rate of the ternary complex formed by SEC3 WT. 3 μM SEC3 WT was mixed with 0, 0.5, 0.75, 1.0, 1.25, 1.75, or 2.25 μM HLA-DR1 and injected over immobilized 14.3.d TCR (2000 RU). A graphical representation of a single exponential fit of the dissociation phases is inserted. The upper part of the insert shows the experimental values as time points and the calculated values as overlaid curves; the lower part displays the corresponding residuals (i.e., the difference between the experimental and calculated values at each time point).

concentrations of soluble HLA-DR1. The sensograms showed a concentration-dependent increase in binding, and the dissociation phases fitted readily to a single exponential equation, yielding k_{off} values of 0.091 ± 0.002 s^{-1} ($t_{1/2}$ = 7.6 s) for wild-type SEC3 and 0.024 ± 0.001 s^{-1} ($t_{1/2}$ = 29 s) for SEC3 3B2. In contrast, the half-life of the ternary complex formed by the 14.3.d β chain alone was far too short to accurately measure by BIAcore. Representative fits (inserts in Figures 4B and 4C) show how remarkably well the data conform to a pseudo-first-order reaction. Thus, increasing the affinity of the SAG-MHC interaction increases the half-life of the ternary complex, as predicted above.

It is noteworthy that the half-lives of the ternary complexes formed by SEC3 and SEC3 3B2 (7.6 and 29 s, respectively) fall within the range measured for specific TCR-peptide/MHC class I or class II complexes (1–60 s) (Corr et al., 1994; Matsui et al., 1994; Alam et al., 1996; Lyons et al., 1996; Kersh et al., 1998). This indicates that the SAG-MHC complex effectively mimics the kinetics of interaction of peptide/MHC with the TCR, even though the binding of SAGs to MHC class II is far weaker than that of specific peptides (Margulies et al., 1996). Stabilization of the TCR-SAG-MHC complex to a level similar to that of the TCR-peptide/MHC complex requires the TCR α chain, since the β chain alone is unable to form ternary complexes of comparable stability.

A Single Amino Acid Change in Vα CDR2 Eliminates the Contribution of the TCR α Chain to Ternary Complex Stabilization

According to our model of the TCR-SEC3-MHC complex (Figure 1), TCR-MHC contacts (<4 Å) are predicted between Vα CDR2 and the MHC β1 helix; this specific interaction should therefore be responsible, at least in part, for the observed stabilization of the ternary complex by the TCR α chain. As shown in Figure 5A, the putative interaction is primarily mediated by Vα CDR2 Ser51 (Li et al., 1998), which is located at the tip of the CDR loop in the crystal structures of the 2C, A6, and B7 TCRs (Garboczi et al., 1996; Garcia et al., 1996; Ding et al., 1998) and that is the most frequently occurring residue at this position in Vα sequences (Arden et al., 1995; Clark et al., 1995). This Vα residue is predicted to contact Thr77 of the HLA-DR1 β chain (Figure 5A), in agreement with the finding that mutations at position 77 of the β chains DR1 and I-E^k have been found to greatly reduce the T cell response to SEB without affecting binding of the SAG to MHC class II (Deckhut et al., 1994; Labrecque et al., 1994). To determine whether Vα CDR2 actually makes any contribution to stabilizing the TCR-SAG-MHC complex, we introduced point mutations at Vα CDR2 positions 49, 51, and 54 of the 2C TCR and tested the effects of these mutations on complex formation. This TCR uses the same Vβ as the 14.3.d TCR (Vβ8.2) but a different Vα (Vα3.1). Unlike Vα CDR2 Ser51, Vα CDR2 Tyr49 and Pro54 are not predicted to

(C) Determination of the off-rate of the ternary complex formed by SEC3 3B. 6 μM SEC3 3B2 was injected over 1800 RU of immobilized 14.3.d TCR in combination with 1.5, 0.91, 0.56, 0.34, 0.21, or 0.13 mM HLA-DR1. Results are presented as in (B).

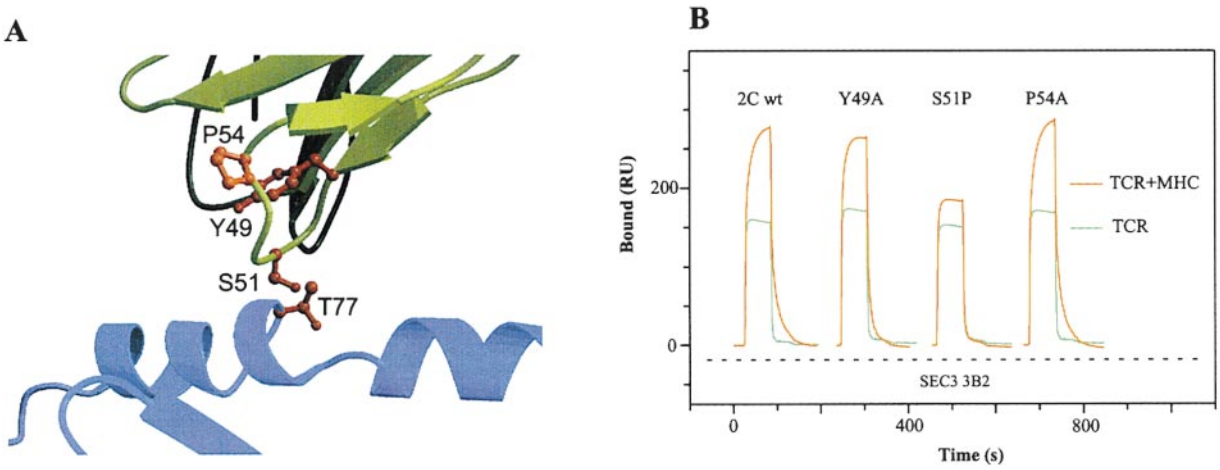

Figure 5. Mutational Analysis of the Role of Vα CDR2 in Stabilizing the TCR-SAG-MHC Complex

(A) Close-up of putative contacts between the Vα domain of the 2C TCR (green) and the α-helix of the HLA-DR1 β1 domain (blue) in the model of the TCR-SEC3-peptide/MHC class II complex in Figure 1. The side chains of Vα CDR2 residues Tyr49, Ser51, and Pro54 and of DR1 β chain residue Thr77 are shown in red.

(B) Equivalent concentrations of wild-type (WT) and mutant (Y49A, S51P, and P54A) 2C TCRs were injected over 500 RU of immobilized SEC3 3B2, either alone (green) or mixed with 0.5 μM HLA-DR1 (red). The identity of each 2C TCR mutant is indicated at the top of each overlay plot.

form direct contacts to MHC in the ternary complex, although they are in proximity to the MHC β1 helix (Figure 5A). A single-chain version of the 2C TCR was expressed in bacterial inclusion bodies and refolded in vitro as described (Schodin et al., 1996; Manning et al., 1998).

Like 14.3.d TCR, wild-type 2C TCR exhibited significantly enhanced binding when injected over immobilized SEC3 3B2 in combination with soluble HLA-DR1 (Figure 5B). The dissociation kinetics for the mixture of 2C TCR and MHC were also clearly slower than for the TCR alone. As noted previously (Manning et al., 1998), immobilization of single-chain 2C TCR to the sensor surface led to its inactivation, which precluded reversing the orientation of the assay, as was possible for 14.3.d TCR. However, our inability to reverse the orientation is not a significant concern in this case, since in contrast to the 14.3.d TCR from *Drosophila* cells, the 2C TCR did not show any signs of aggregation when injected alone over the immobilized SAG: the equilibrium binding level was reached within seconds and the response rapidly returned to baseline upon completion of the injection (compare Figures 2A and 5B).

We next compared the binding of wild-type 2C TCR to immobilized SEC 3B2 with that of three point mutants in Vα CDR2: Y49A, S51P, and P54A. The Vα S51P substitution is one of three naturally occurring amino acid differences between Vα3.1 and Vα3.2 that are known to influence CD4/CD8 lineage commitment (Sim et al., 1996). After serine and threonine, proline is the most frequently occurring residue at position 51 in mouse Vα regions (8% of all sequences, compared with 53% for serine and 28% for threonine) (Clark et al., 1995). As expected from the crystal structure of the TCR β-SEC3 complex (Fields et al., 1996), these mutations did not affect the affinity of the 2C TCR for SEC3 alone (data not shown). To permit a quantitative comparison, wild-type and mutant TCRs were first titrated on immobilized SEC3 3B2 in order to obtain the same amount of bound protein for each (Figure 5B). The experiment was then repeated using equivalent amounts of TCR in the presence of a fixed concentration (0.5 μM) of soluble HLA-DR1. The Vα Y49A mutation resulted in a small, though detectable, effect on ternary complex formation. The kinetics were slightly different than those of wild-type 2C TCR: the association phase reached a plateau sooner and the off-rate was more rapid. The maximum response was also somewhat reduced compared with wild-type. In contrast, the Vα S51P mutant displayed an almost complete loss of enhanced binding and the off-rate was unaffected by the addition of HLA-DR1. Indeed, the sensograms obtained for Vα S51P in the presence or absence of DR1 closely resemble those in Figure 2B for the binding of isolated 14.3.d β chain to immobilized SEC3, with or without MHC. Finally, the Vα P54A mutation had no detectable effect on complex formation. Thus, a single mutation at position 51 of Vα CDR2 is sufficient to eliminate the contribution of the α chain to stabilization of the TCR-SAG-MHC complex, whereas mutations at Vα CDR2 positions 49 or 54 have little or no effect. These results are consistent with our model of the ternary complex (Figure 1) in which Vα Ser51, located at the tip of the CDR2 loop, contacts the HLA-DR1 β1 helix, but in which Vα Ty49 and Pro54, although also part of the loop, do not participate in direct interactions with MHC (Figure 5A).

Although we do not know whether the serine-to-proline substitution at position 51 of the 2C TCR α chain would reduce the reactivity to SEC3 or SEB of a T cell bearing the mutant TCR, Smith et al. (1992) reported that Vβ8.1$^+$ hybridomas expressing Vα11.1 were SEB reactive, whereas Vβ8.1$^+$ hybridomas expressing Vα11.3 were not. Since SEB is likely to bind Vβ8.1 in the same manner as Vβ8.2 (the sequences of the two β chains are 90% identical), the Vα domain of TCRs expressing Vβ8.1 should be oriented similarly with respect to the

MHC β1 helix as the Vα3.1 domain of the 2C TCR in the model of the TCR-SAG-MHC complex in Figure 1. A comparison of the amino acid sequences of Vα11.1 and Vα11.3 reveals that Vα11.1, like wild-type 2C α chain, has a serine at position 51. However, Vα11.3 has a proline at this position, as does the 2C TCR mutant that does not exhibit α chain-mediated stabilization of the TCR-SAG-MHC complex. The only other difference in the CDR2 sequences of Vα11.1 and Vα11.3 is a conservative alanine-to-valine substitution at position 50.

Conclusions

We have shown that the TCR α chain is required for maximum stabilization of the TCR-SAG-MHC complex and that the α chain increases the half-life of the complex to a value comparable to those reported for TCR-peptide/MHC class I or class II complexes (Corr et al., 1994; Matsui et al., 1994; Alam et al., 1996; Lyons et al., 1996; Kersh et al., 1998). Since different TCR α chains can be expected to stabilize the TCR-SAG-MHC complex to different extents, this may explain the preferential expression of certain Vα regions observed among T cells reactive with a particular SAG. We have also demonstrated that increasing the affinity of the SEC3-DR1 interaction further stabilizes the TCR-SAG-MHC complex, as predicted by a model involving direct TCR-MHC interactions. By showing that a single amino acid change at position 51 of Vα CDR2 eliminates the contribution of the α chain to ternary complex stabilization, we have identified this CDR as the likely site of interaction with MHC.

It is probably not coincidental that the half-life of the TCR-SEC3-MHC class II complex falls within the range measured for specific TCR-peptide/MHC complexes. This implies that SAGs have evolved to mimic the kinetics of interaction of peptide/MHC complexes with the TCR. To do so, SAGs have developed a novel strategy to compensate for their relatively low (compared with antigenic peptides) affinities for MHC. This involves cross-linking TCR and MHC in such a way that the TCR Vα domain is brought into proximity of the MHC class II β1 domain, permitting direct TCR-MHC interactions that further stabilize the ternary complex. It is noteworthy that the rotational orientation of TCR and MHC molecules in our model of the TCR-SEB-MHC complex (Li et al., 1998) differs by about 40° from that in the TCR-peptide/MHC complex (Garboczi et al., 1996; Ding et al., 1998; Garcia et al., 1998) and that there are no direct contacts between the TCR β chain and MHC or between bound peptide and the TCR combining site (Figure 1). This indicates that the specific geometry of TCR engagement by a particular ligand may be less critical for T cell activation than certain other factors, in particular the stability of the resulting complex (Kersh et al., 1998). It should be emphasized, however, that the half-lives of both TCR-SAG-MHC and TCR-peptide/MHC complexes are far shorter than those reported for other ligand-receptor complexes (e.g., antigen-antibody, homone-hormone receptor, and cytokine-cytokine receptor), whose half-lives are measured in minutes or hours rather than seconds. Indeed, the serial triggering (Valitutti et al., 1995; Viola and Lanzavecchia, 1996) and kinetic proofreading (Rabinowitz et al., 1996) models of T cell activation argue that the short half-lives of TCR-peptide/MHC or TCR-SAG-MHC complexes are necessary to enable a single ligand to serially engage a large number of TCRs. It remains to be established, however, whether ligands that form complexes with very long half-lives (minutes or hours) are actually less efficient at triggering T cells or whether ligands that form progressively more stable complexes stimulate T cells increasingly well, until some plateau of maximum stimulation is attained.

Experimental Procedures

Protein Expression and Purification

Soluble 14.3.d TCR β chain was produced in J558L myeloma cells and affinity purified as previously described (Bentley et al., 1995) using the anti-mouse Cβ monoclonal antibody H57-597 (Kubo et al., 1989). Soluble 14.3.d αβ TCR heterodimer was produced in *Drosophila* cells basically as described (Wallny et al., 1995). The recombinant protein was purified from culture supernatants using antibody H57-597, followed by gel filtration on a Superdex 200 column (Pharmacia Biotech AB, Uppsala, Sweden) immediately before BIAcore experiments to eliminate aggregated material that could interfere with affinity measurements. The 14.3.d αβ TCR was also purified by gel filtration before BIAcore. Wild-type and mutant 2C single-chain TCRs were constructed as thioredoxin fusion proteins with a His_6 tag, using a PCR-based technique (Manning et al., 1998). Proteins were expressed in *E. coli* strain GI698 and isolated from inclusion bodies by denaturing affinity chromatography using His-Bind resin (Novagen). Following renaturation by dialysis (Schodin et al., 1996), the monomeric proteins were purified by gel filtration on a Superdex 200 column. Soluble HLA-DR1 was produced as previously described (Stern and Wiley, 1992; Murthy and Stern, 1997; Leder et al., 1998) using a recombinant baculovirus (pACDR1) encoding both DRα and DRβ1*0101 chains. The empty αβ DR1 heterodimer was loaded with peptides HA 306-318 or YAK as described (Stern and Wiley, 1992). Recombinant wild-type SEC3 was prepared from *Staphylococcus aureus* strain FRI913 as described (Blomster-Hautamaa and Schlievert, 1988).

Phage Display and Affinity Maturation of SEC3

To obtain SEC3 variants with enhanced affinity for HLA-DR1, SEC3 residues 43–47 (KFLAH) were randomized using degenerate oligonucleotides PCR, and the resulting phage library selected by panning on immobilized DR1 molecules. To construct the library, the SEC3 gene was first amplified from a plasmid that harbors the gene in its genomic configuration (Hovde et al., 1990) and subcloned into the pCANTAB-5E vector (Pharmacia Biotech AB) using appropiate DNA modifying enzymes. A single clone (pSEC3 WT) was chosen and used as template in subsequent PCR procedures. The N-terminal part of SEC3 was amplified with Vent DNA polymerase (New England Biolabs) using primers PSA012 (AATTATTATTCGCAATTCC TTTAG, matching the pelB leader sequence) and PSA027 (GTTATAA ATTAAATCSNNSNNSNNSNNSNNATCTACAGACATAA C, matching the anti-sense strand of the region to be randomized). The C-terminal part of the gene was similarly amplified using primers PSA026 (AAAGTTATGTCTGTAGATNNSNNSNNSNNSNNSGATTTAATTTAT AAC, matching the sense strand of the area to be randomized) and PSA023 (ACTTTCAACAGTCTATGCGGC, complementary to the sequence of phage gene III located just downstream of the SEC3 gene). The two PCR products (215 and 678 bp, respectively) were gel purified and joined by PCR overlap extension using the flanking primers PSA011 and PSA023. The full product (845 bp) was purified, digested with SfiI and NotI, and ligated into pCANTAB-5E. The ligated DNA was purified and electroporated into *E. coli* strain TG1.

The preparation of phage for selection experiments was carried out essentially as described (Marks et al., 1991). The library was selected using soluble HLA-DR1 immobilized on MaxiSorp plastic microtiter plates (NUNC A/C, Roskilde, Denmark). MHC was diluted to 20 μg/ml in PBS, and 200 μl was applied to four wells in a microtiter plate. The plate was left overnight at 4°C. After blocking the wells by filling them completely with PBS containing 2% skimmed milk powder (SMP-PBS), 80 μl phage stock diluted 1:1 in

SMP-PBS (approximately 5×10^{12} cfu) was applied to each HLA-DR1-coated well. The plate was slowly rotated at room temperature at an angle of about 80° for 1.5 hr. Unbound phage were removed by 10 washes with PBS containing 0.005% Tween-20 (PBS/Tween), followed by 10 washes with PBS alone. Bound phage were eluted by incubation with 200 μl 0.1 M glycine-HCl (pH 2.2) for 10 min. The eluate was immediately neutralized with 7 μl 2 M Tris base; half of the eluate was used to infect log phase TG1 cells. An aliquot was removed for titration after 1 hr at 37°C to estimate the amount of infected cells, and the remaining cells were transferred into fresh medium and grown to an optical density of 0.5–0.8. Helper phage were added and the superinfection procedure performed as described above. The resulting phage were used for further selection. Two additional rounds of panning were carried out using only one HLA-DR1-coated well. In the final round, the stringency was increased by repeating the PBS/Tween wash 30 times. Initial testing of selected clones for binding to sHLA-DR1 was done by whole phage ELISA. Single colonies from the third round of selection were grown in a microtiter format to mid-log density and superinfected (Marks et al., 1991). Phage supernatants were tranferred to ELISA plates precoated with sHLA-DR1 and incubated for 2 hr at room temperature. The plates were washed three times with PBS/Tween, and bound phage were detected using a peroxidase-conjugated anti-M13 antibody (Pharmacia Biotech AB) according to the manufacturer's instructions.

To produce soluble SEC3 mutants, phagemid DNA of selected clones was transfected into *E. coli* nonsuppressor strain HB 2151 (Hoogenboom et al., 1991). Protein synthesis was induced by adding 1 mM isopropyl β-D-thiogalactoside to bacteria grown to mid-log density at 37°C. The periplasmic fraction was harvested by osmotic shock (Skerra and Pluckthun, 1988) after an additional 3–6 hr of growth at 37°C. Protein was purified as described by Leder et al. (1998) using RedA-Dye affinity chromatography (Amicon). Yields of SEC3 mutants (>95% pure as judged by SDS-PAGE) were typically 2–5 mg per liter of bacterial culture.

BIAcore Analysis

Binding studies were conducted by surface plasmon resonance detection using a BIAcore 1000 instument (BIAcore). Prior to immobilization, ligands were dialyzed against 10 mM sodium acetate, (pH 5.0–5.5) and diluted to about 50 μg/ml. Couplings to the dextran matrix of the CM-5 sensor chip were done using standard amine coupling chemistry. Experiments were conducted at 25°C in 10 mM Hepes, 3.4 mM EDTA, 150 mM NaCl, and 0.005% Surfactant P-20 (pH 7.5). Proteins were either dialyzed against HBS (SAGs and 2C TCR mutants) or purified by size-exclusion chromatography using HBS as running buffer (HLA-DR1, 14.3.d TCR and corresponding β chain), prior to BIAcore analysis.

Qualitative studies of complex formation (results presented in Figures 2, 4A, and 5B) were done at a flow rate of 5 ml/min using the Quickinject command to inject sample into the flow cell. Chip surfaces coupled with SAGs were regenerated with 10 mM HCl when needed. Since immobilized TCR and β chain were highly sensitive to acid, regenerations were carried out by continuous washing with HBS until the signal reached baseline values.

Affinities of HLA-DR1 for wild-type SEC3 and SEC3 mutants were determined by Scatchard analysis using the same basic experimental conditions as above, except for the addition of 20 mM $ZnCl_2$ to the HBS. Soluble HLA-DR1 was captured by passage over immobilized SEA; injections of each SAG (wild-type SEC3, SEC3 3B1, and SEC3 3B2) were then done serially at fixed time points. The chip was regenerated between each MHC injection by extensive washing with HBS (without Zn^{2+}). Blank runs were done on the SEA-coupled chip prior to the injection of MHC. Kinetic analysis was performed at increased flow rate (15 μl/min) and decreased chip densities (less than 1000 RU of active TCR) using the Kinject command to inject sample into the flow cell. Faster flow rates or lower chip densities had no effect on the dissociation phase. BIAcore data was converted into ASCII text files and analyzed on an IBM compatible PC using the GraFit software (Microsoft)

T Cell Proliferation Assay

Lymph node T cells (4×10^4) from RAG-$2^{-/-}$ TCR transgenic mice expressing the 14.3.d TCR (Kirkberg et al., 1994) were cultured together with 2×10^5 irradiated (10,000 rad) mouse L cells expressing HLA-DR1 as APC in the presence of varying amounts of different SAGs in 200 μl of IMDM supplemented with 10% FCS as duplicates in flat-bottom 96-well plates. Syngeneic APCs were removed Dynabeads (Dynal A/S, Oslo, Norway) coated with the anti-MHC class II monoclonal antibody M5/114 (Bhattacharya et al., 1981). After 48 or 72 hr of incubation at 37°C, 1 μCi/well of [^{3}H]thymidine was added for the next 12 hr. Incorporation of radioactivity was then measured using a Betaplate 1250 system (Wallacy, Turku, Finland).

Acknowledgments

This research was supported by National Institutes of Health (NIH) grants AI36900 and AI42937 and National Multiple Sclerosis Society grant RG2747 (R. A. M.), NIH grant HL36611 (P. M. S.), NIH grant GM55767 (D. M. K.), and grants from the National Cancer Institute of Canada (R.-P. S.). Support from the Lucille P. Markey Charitable Trust is also gratefully acknowledged. We thank I. A. Wilson for coordinates of the 2C TCR-dEV8/H-2K^b complex, L. J. Stern for the pACDR1 baculovirus vector used for producing soluble HLA-DR1, T. Manning and E. Parke for their assistance with the Vα mutants, and E. Eisenstein for helpful discussions. The Basel Institute for Immunology was founded and is supported by F. Hoffmann-LaRoche Ltd., Basel, Switzerland. R.-P. S. holds a Medical Research Council of Canada Scientist Award. P. M. L. is supported by the Medical Research Council of Canada. P. S. A. is a Fellow of the Danish Natural Science Research Council.

Received February 10, 1999; revised March 8, 1999.

References

Abrahmsen, L., Dohlsten, M., Segren, S., Bjork, P., Jonsson, E., and Kalland, T. (1995). Characterization of two distinct MHC class II binding sites in the superantigen staphylococcal enterotoxin A. EMBO J. *14*, 2978–2986.

Alam, S.M., Travers, P.J., Wung, J.L., Nasholds, W., Redpath, S., Jameson, S.C., and Gascoigne, N.R.J. (1996). T-cell receptor affinity and thymocyte positive selection. Nature *381*, 616–620.

Arden, B., Clark, S.P., Kabelitz, D., and Mak, T.W. (1995). Human T-cell receptor variable gene segment families. Immunogenetics *42*, 455–500.

Bentley, G.A., Boulot, G., Karjalainen, K., and Mariuzza, R.A. (1995). Crystal structure of the β chain of a T cell antigen receptor. Science *267*, 1984–1987.

Bhattacharya, A., Dorf, M.E., and Springer, T.A. (1981). A shared alloantigenic determinant on Ia antigens encoded by the I-A and I-E subregions: evidence for I region gene duplication. J. Immunol. *127*, 2488–2495.

Blackman, M.A., and Woodland, D.L. (1996). Role of the T cell receptor α-chain in superantigen recognition. Immunol. Res. *15*, 98–113.

Blackman, M.A., Gerhard-Burgert, H., Woodland, D.L., Palmer, E., Kappler, J.W., and Marrack, P. (1990). A role for clonal inactivation in T cell tolerance to Mls-1a. Nature *345*, 540–542.

Blomster-Hautamaa, D.A., and Schlievert, P.M. (1988). Preparation of toxic shock syndrome toxin-1. Methods Enzymol. *165*, 37–42.

Bohach, G.A. (1997). Staphylococcal enterotoxins B and C: structural requirements for superantigenic and entertoxigenic activities. In Superantigens: Molecular Biology, Immunology and Relevance to Human Disease, D.Y.M. Leung, B.T. Huber, and P.M. Schlievert, eds. (New York: Marcel Dekker Inc.), pp. 167–198.

Bohach, G.A., Fast, D.J., Nelson, R.D., and Schlievert, P.M. (1990). Staphylococcal and streptococcal pyrogenic toxins involved in toxic shock syndrome and related illnesses. Crit. Rev. Microbiol. *17*, 251–272.

Borrero, H., Donson, D., Cervera, C., Rexer, C., and Macphail, S. (1995). T cell receptor Vα4 is expressed by a subpopulation of Vβ6 T cells that respond to the bacterial superantigen staphylococcal enterotoxin B. J. Immunol. *154*, 4247–4260.

Clark, S.P., Arden, B., Kabelitz, D., and Mack, T.W. (1995) Comparison of human and mouse T-cell receptor variable gene segment subfamilies. Immunogenetics *42*, 531–540.

Corr, M., Slanetz, A.E., Boyd, L.F., Jelonek, M.T., Khilko, S., Al-Ramadi, B.K., Kim, Y.S., Maher, S.E., Bothwell, A.L., and Margulies, D.H. (1994). T cell receptor-MHC class I peptide interactions: affinity, kinetics, and specificity. Science *265*, 946–948.

Daly, K., Nguyen, P., Hankley, D., Zhang, W.J., Woodland, D.L., and Blackman, M.A. (1995). Contribution of the TCR α-chain to the differential recognition of bacterial and retroviral superantigens. J. Immunol. *155*, 27–34.

Davis, S.J., Ikemizu, S., Wild, M.K., and van der Merwe, P.A. (1998). CD2 and the nature of protein interactions mediating cell-cell recognition. Immunol. Rev. *163*, 217–236.

Deckhut, A.M., Chien, Y., Blackman, M.A., and Woodland, D.L. (1994). Evidence for a functional interaction between the β chain of major histocompatibility complex class II and the T cell receptor α chain during recognition of a bacterial superantigen. J. Exp. Med. *180*, 1931–1935.

Dessen, A., Lawrence, C.M., Cupo, S., Zaller, D.M., and Wiley, D.C. (1997). X-ray crystal structure of HLA-DR4 (DRA*0101, DRB1*0401) complexed with a peptide from human collagen II. Immunity *7*, 473–481.

Ding, Y.-H., Smith, K.J., Garboczi, D.N., Utz, U., Biddison, W.E., and Wiley, D.C. (1998). Two human T cell receptors bind in a similar diagonal mode to the HLA-A2/Tax peptide complex using different TCR amino acids. Immunity *8*, 403–411.

Donson, D., Borrero, H., Rutman, M., Pergolizzi, R., Malhado, N., and Macphail, S. (1997). Gene transfer directly demonstrates a role for TCR Vα elements in superantigen recognition. J. Immunol. *158*, 5229–5236.

Fields, B.A., Malchiodi, E.L., Li, H.-M., Ysern, X., Stauffacher, C.V., Schlievert, P.M., Karjalainen, K., and Mariuzza, R.A. (1996). Crystal structure of the β chain of a T-cell receptor complexed with a superantigen. Nature *384*, 188–192.

Garboczi, D.N., Ghosh, P., Utz, U., Fan, Q.R., Biddison, W.E., and Wiley, D.C. (1996). Structure of the complex between human T-cell receptor, viral peptide and HLA-A2. Nature *384*, 134–141.

Garcia, K.C., Degano, M., Stanfield, R.L., Brunmark, A., Jackson, M.R., Peterson, P.A., Teyton, L., and Wilson, I.A. (1996). An $\alpha\beta$ T cell receptor structure at 2.5 Å and its orientation in the TCR-MHC complex. Science *274*, 209–219.

Garcia, K.C., Degano, M., Pease, L.R., Huang, M., Peterson, P.A., Teyton, L., and Wilson, I.A. (1998). Structural basis of plasticity in T cell receptor recognition of a self peptide-MHC antigen. Science *279*, 1166–1172.

Gascoigne, N.R.J., and Ames, K.T. (1991). Direct binding of secreted T-cell receptor β chain to superantigen associated with class II major histocompatibility complex protein. Proc. Natl. Acad. Sci. USA *88*, 613–616.

Hoffmann, M.L., Jablonski, L.M., Crum, K.K., Hackett, S.P., Chi, Y.-I., Stauffacher, C.V., Stevens, D.L., and Bohach, G.A. (1994). Predictions of T cell receptor and major histocompatibility complex binding sites on staphylococcal enterotoxin C3. Infect. Immun. *62*, 3396–3407.

Hoogenboom, H.R., Griffiths, A.D., Johnson, K.S., Chiswell, D.J., Hudson, P., and Winter, G. (1991). Multi-subunit proteins on the surface of filamentous phage: methodologies for displaying antibody (Fab) heavy and light chains. Nucleic Acids Res. *19*, 4133–4137.

Housset, D., Mazza, G., Gregoire, C., Piras, C., Malissen, B., and Fontecilla-Camps, J.C. (1997). The three-dimensional structure of a T-cell antigen receptor VαVβ heterodimer reveals a novel arrangement of the Vβ domain. EMBO J. *16*, 4205–4216.

Hovde, C.J., Hackett, S.P., and Bohach, G.A. (1990). Nucleotide sequence of the staphylococcal enterotoxin C3: sequence comparison of all three type C staphylococcal enterotoxins. Mol. Gen. Genet. *220*, 329–333.

Hudson, K.R., Tiedemann, R.E., Urban, R.G., Lowe, S.C., Strominger, J.L., and Fraser, J.D. (1995). Staphylococcal enterotoxin A has two cooperative binding sites on major histocompatibility complex class II. J. Exp. Med. *182*, 711–720.

Jardetzky, T.S., Brown, J.H., Gorga, J.C., Stern, L.J., Urban, R.G., Chi, Y., Stauffacher, C., Strominger, J.L., and Wiley, D.C. (1994). Three-dimensional structure of a human class II histocompatibility molecule complexed with superantigen. Nature *368*, 711–718.

Kersh, G.J., Kersh, E.N., Fremont, D.H., and Allen, P.M. (1998). High- and low-potency ligands with similar affinities for the TCR: the importance of kinetics in TCR signaling. Immunity *9*, 817–826.

Kim, J., Urban, R.G., Strominger, J.L., and Wiley, D.C. (1994). Toxic shock syndrome toxin-1 complexed with a class II major histocompatibility molecule HLA-DR1. Science *266*, 1870–1874.

Kirkberg, J., Baron, S., Jakob, S., Rolink, A., Karjalainen, K., and von Boehmer, H. (1994). Thymic selection of $CD8^+$ single positive cells with a class II major histocompatibility complex-restricted receptor. J. Exp. Med. *180*, 25–34.

Kotzin, B.L., Leung, D.Y.M., Kappler, J., and Marrack, P. (1993). Superantigens and their potential role in human disease. Adv. Immunol. *54*, 99–166.

Kozono, H., Parker, D., White, J., Marrack, P., and Kappler, J. (1995). Multiple binding sites for bacterial superantigens on soluble class II molecules. Immunity *3*, 187–196.

Kubo, R.T., Born, W., Kappler, J.W., Marrack, P., and Pigeon, M. (1989). Characterization of a monoclonal antibody which detects all murine $\alpha\beta$ T cell receptors. J. Immunol. *142*, 2736–2742.

Labrecque, N., Thibodeau, J., Mourad, W., and Sékaly, R.-P. (1994). T cell receptor-major histocombatibility complex class II interaction is required for the T cell response to bacterial superantigens. J. Exp. Med. *180*, 1921–1929.

Leder, L., Llera, A., Lavoie, P.M., Lebedeva, M.I., Li, H., Sékaly, R.-P., Bohach, G.A., Gahr, P.J., Schlievert, P.M., Karjalainen, K., et al. (1998). A mutational analysis of the binding of staphylococcal enterotoxins B and C3 to the T cell receptor β chain and major histocompatibility complex class II. J. Exp. Med. *187*, 823–833.

Li, H., Llera, A., Tsuchiya, D., Leder, L., Ysern, X., Schlievert, P.M., Karjalainen, K., and Mariuzza, R.A. (1998). Three-dimensional structure of the complex between a T cell receptor β chain and the superantigen staphylococcal enterotoxin B. Immunity *9*, 807–816.

Li, H., Llera, A., Malchiodi, E.L., and Mariuzza, R.A. (1999). The structural basis of T cell activation by superantigens. Annu. Rev. Immunol. *17*, 435–466.

Lyons, D.S., Lieberman, S.A., Hampl, J., Boniface, J.J., Chien, Y.-H., Berg, L.J., and Davis, M.M. (1996). A TCR binds to antagonist ligands with lower affinities and faster dissociation rates than to agonists. Immunity *5*, 53–61.

Malchiodi, E.L., Eisenstein, E., Fields, B.A., Ohlendorf, D.H., Schlievert, P.M., Karjalainen, K., and Mariuzza, R.A. (1995). Superantigen binding to a T cell receptor β chain of known three-dimensional structure. J. Exp. Med. *182*, 1833–1845.

Manning, T.C., Schlueter, C.J., Brodnicki, T.C., Parke, E.A., Speir, J.A., Garcia, K.C., Teyton, L., Wilson, I.A., and Kranz, D.M. (1998). Alanine scanning mutagenesis of an $\alpha\beta$ T cell receptor: mapping the energy of antigen recognition. Immunity *8*, 413–425.

Margulies, D.H., Plaskin, D., Khilko, S.N., and Jelonek, M.T. (1996). Studying interactions involving the T-cell antigen receptor by surface plasmon resonance. Curr. Opin. Immunol. *8*, 262–270.

Marks, J.D., Hoogenboom, H.R., Bonnert, T.P., McCaffery, J., Griffiths, A.D., and Winter, G. (1991). By-passing immunization. Human antibodies from V-gene libraries displayed on phage. J. Mol. Biol. *222*, 581–597.

Matsui, K., Boniface, J.J., Steffner, P., Reay, P.A., and Davis, M.M. (1994). Kinetics of T cell receptor binding to peptide/I-E^k complexes: correlation of the dissociation rate with T-cell responsiveness. Proc. Natl. Acad. Sci. USA *91*, 12862–12866.

Murthy, V.L., and Stern, L.J. (1997). The class II MHC protein HLA-DR1 in complex with an endogenous peptide: implications for the structural basis of the specificity of peptide binding. Structure *5*, 1385-1396.

Natarajan, S.K., Stern, L.J., and Sadegh-Nasseri, S. (1999). SDS-stability of HLA-DR1 complexes correlates with burial of hydrophobic residues in pocket 1. J. Immunol., in press.

Proft, T., and Fraser, J. (1998). Superantigens: just like peptides only different. J. Exp. Med. *187*, 819–821.

Rabinowitz, J.D., Beeson, C., Lyons, D.S., Davis, M.M., and McConnell, H.M. (1996). Kinetic discrimination in T-cell activation. Proc. Natl. Acad. Sci. USA *93*, 1401–1405.

Scherer, M.T., Ignatowicz, L., Winslow, G.M., Kappler, J.W., and Marrack, P. (1993). Superantigens: bacterial and viral proteins that manipulate the immune system. Annu. Rev. Cell. Biol. *9*, 101–128.

Schodin, B.A., Schlueter, C.J., and Kranz, D.M. (1996). Binding properties and solubility of single-chain T cell receptors expressed in *E. coli*. Mol. Immunol. *33*, 819–829.

Seth, A., Stern, L.S., Ottenhoff, T.H.M., Engel, I., Owen, M.J., Lamb, J.R., Klausner, R.D., and Wiley, D.C. (1994). Binary and ternary complexes between T-cell receptor, class II MHC and superantigen *in vitro*. Nature *369*, 324–327.

Sim, B.-C., Zerva, L., Greene, M.I., and Gascoigne, N.R.J. (1996). Control of MHC restriction by TCR Vα CDR1 and CDR2. Science *273*, 963–966.

Skerra, A., and Pluckthun, A. (1988). Assembly of a functional immunoglobulin Fv fragment in *Escherichia coli*. Science *240*, 1038–1041.

Smith, H.P., Le, P., Woodland, D.L., and Blackman, M.A. (1992). T cell receptor α-chain influences reactivity to Mls-1 in Vβ8.1 transgenic mice. J. Immunol. *149*, 887–896.

Stern, L.J., and Wiley, D.C. (1992). The human class II MHC protein HLA-DR1 assembles as empty αβ heterodimers in the absence of antigenic peptide. Cell *68*, 465–477.

Swaminathan, S., Furey, W., Pletcher, J., and Sax, M. (1992). Crystal structure of staphylococcal enterotoxin B, a superantigen. Nature *359*, 801–806.

Tiedemann, R.E., Urban, R.J., Strominger, J.L., and Fraser, J.D. (1995). Isolation of HLA-DR1.(staphylococcal enterotoxin A)$_2$ trimers in solution. Proc. Natl. Acad. Sci. USA *92*, 12156–12159.

Valitutti, S., Muller, S., Cella, M., Padovan, E., and Lanzavecchia, A. (1995). Serial triggering of many T-cell receptors by a few peptide-MHC complexes. Nature *375*, 148–151.

Viola, A., and Lanzavecchia, A. (1996). T cell activation determined by T cell receptor number and tunable thresholds. Science *273*, 104–106.

Wang, J., Lim, K., Smolyar, A., Teng, M., Liu, J., Tse, A.G.D., Liu, J., Hussey, R.E., Chishti, Y., Thomson, C.T.T., et al. (1998). Atomic structure of an αβ T cell receptor (TCR) heterodimer in complex with an anti-TCR Fab fragment derived from a mitogenic antibody. EMBO J. *17*, 10–26.

Webb, S.R., and Gascoigne, N.R.J. (1994). T-cell activation by superantigens. Curr. Opin. Immunol. *6*, 467–475.

Wallny, H.-J., Solami, G., and Karjalaien, K. (1995). Soluble mouse major histocompatibility complex class II molecules produced in Drosophila cells. Eur. J. Immunol. *25*, 1262–1266.

Woodland, D.L., and Blackman, M.A. (1993). How do T cell receptors, MHC molecules and superantigens get together? Immunol. Today *14*, 208–212.